

International Conference on Global Trends in Pure and Applied Chemical Sciences 2017

Invitation Letter

14-10-2017

To: KHALID JAWAD KADHIM

Address: COLLEGE OF EDUCATION, UNIVERSITY OF AL-QADISIYAH, AL DIWANEYAH

Country: Iraq

Passport no. A12268095

Dear Delegate,

It gives us immense pleasure in inviting you to attend the "3rd INTERNATIONAL CONFERENCE ON GLOBAL TRENDS IN PURE AND APPLIED CHEMICAL SCIENCES - 2017", to be organized by SRM University (Delhi NCR Campus) & Asian Publication Corporation (Asian Journal of Chemistry), which will be held on December 8-9, 2017 at SRM University (Delhi NCR Campus).

Your article entitled: **Synthesis, Spectral Characterization and Biological Studies of new Heterocyclic Azo-Schiff Base Compound (E)-5-((E)-(1H-benzo[d]imidazol-2-yl)diazanyl)-N-(4-chlorobenzylidene)-2-amine-4,6-dimethylpyridin with some Metal Ions**, has been accepted for POSTER presentation in 3rd ICGTCS-2017.

This Professional and Scholarly gathering of over 250 attendees will feature more than 20 plenary, keynote and invited lecture presentations in various sessions throughout the conference. We look forward to offer you a warm welcome and assure a stimulating program of scientific papers and plenary sessions. Additional information about the conference is available on the website:

<http://icgtcs-2017.asianjournalofchemistry.co.in/about%20us.html>

It will be a personal pleasure to host you in Delhi and I will look forward to it. Please feel free to contact me any time if there is anything that we can do to facilitate your visit.

Kindest regards

Mrs. Anjul Agarwal
Organizing Secretary
ICGTCS-2017

<http://icgtcs-2017.asianjournalofchemistry.co.in/>

Conference Secretariat
ICGTCS-2017

ASIAN JOURNAL OF CHEMISTRY

11/100, Rajendra Nagar, Sector-3, Sahibabad-201005 (Ghaziabad) INDIA

Tel: 0120-4101551, 4154793

E-mail: asianicgtc-2017@gmail.com



Save to my Dropbox

Synthesis, Spectral Characterization and Biological Studies of new Heterocyclic Azo-Schiff Base Compound (E)-5-((E)-(1H-benzo[d]imidazol-2-yl)diazenyl)-N-(4-chlorobenzylidene)-2-amine-4,6-dimethylpyridin with some Metal Ions

Khalid J. Al-Adilee and Haitham K. Dakheel

Department of Chemistry, College of Education, University of Al-Qadisiyah, Diwaniya 1753, Iraq
*Corresponding author: Prof. Dr. Khalid J. Al-Adilee, Dean of college of Education, E-mail: -Khalidke.1962@yahoo.com; khalid.jawad@qu.edu.iq

Abstract

In this study, new azo-azomethine ligand L_2 and their complexes were synthesized and characterized by the analytical and spectroscopic methods analytical methods such as elemental analysis, molar conductance measurements, magnetic susceptibility, Mass spectral, ^1H -NMR, FT-IR, UV-Visb., TGA, SEM and X-ray diffraction studies. Spectral studies suggest the mole ratio $[\text{M}:\text{L}]$ was $[1:2]$ for $\text{Cu}(\text{II})$ metal ion and $[1:1]$ for $\text{Ag}(\text{I})$ and $\text{Au}(\text{III})$ metal ions. The structures of these complexes were elucidated on the basis of different techniques suggest the structures of the prepared metal complexes octahedral geometry for the $\text{Cu}(\text{II})$ complex and tetrahedral geometry of $\text{Ag}(\text{I})$ complex and square planar geometry for the $\text{Au}(\text{III})$ complex. Their antimicrobial activity against *Escherichia coli* and *Staphylococcus aureus* was performed. Only complex $[\text{Cu}(\text{L}_2)_2\text{Cl}_2] \cdot \text{H}_2\text{O}$ is showed quite effective against tested bacteria. The study assessed the synthesized compounds for their anticancer features against one human cancer cell lines (PC3). Furthermore, the cytotoxicity of the synthesized compound was experimented by using a normal human cell line. The complex $[\text{Ag}(\text{L}_2)(\text{ONO}_2)(\text{H}_2\text{O})]$ prevented the spread of the PC3 cancer cells with a medium inhibitory concentration (IC_{50}) values of $425 \mu\text{M}$. Hence, the outcomes of the study revealed that the $\text{Ag}(\text{I})$ - complexes of L_2 might present a new route for developing cancer chemotherapies to cure PC3 malignancies in human beings.

Key words :- Synthesis, azo-schiff base, Metal Complexes, X-ray diffraction, TGA and SEM, spectral studies, Biological activity

Introduction

Azo-azomethines are seen as organic dyes which consist of the characteristic chromophore groups $-N=N-$ and $-CH=N-$. The azo group is featured by its capacity to formulate a harmonized bonds with the different metal ions [1]. As far as Azo-Schiff bases are concerned, they have an ability to shape coordinate links with numerous metal ions via Azo and azomethine nitrogen atom and extra donor atoms such as O and S [2]. Many of Azo-Schiff base dyes are used as chromogenic reagents for colorimetric purposes and as signs for complexometric titration [3]. Besides, some Azo-Schiff base are shown have to effective antimicrobial behaviours [4]. Because of their different biological actions like anti-tumor and fungicidal, Azo-schiff bases and their complexes are significant [5,6]. Being a malignant tumor or malignant neoplasm, Cancer is a kind of diseases that is featured by its uncontrollable growth of cell. Annually, a great number of people are diagnosed with cancer, and its majority of cases have led to death. Thus, numerous strategies are explored to suppress its malignancy [7]. Complexes containing metal ions with valence electron configuration d^{10} are known to have anticancer effect because of their covalent interaction with DNA and enzyme activity inhibition [8]. The main representatives of this anti-cancer class of drugs are the Pt(II)-based compounds, cis-platin and carbo-platin, which are widely used in current cancer chemotherapy protocols [9]. Recently, there has been a growing concern in the use of Ag(I) compounds in cancer chemotherapy [10]. This concern might be attributed to two reasons. First, Ag(I) center is isoelectronic to Au(I)-complexes and assume tetrahedral structure. Second, Ag(I)-complexes have shown powerful tumor cell growth inhibitory roles by a non-cis-platin-like type of action. However, Au(I)-complexes high redox potentiality and their instability make their application under physiological circumstances problematic. Latest studies in this regards have shown that the Ag(I)-complexes are attained while they are stable under physiological conditions, revealing cytotoxic features to numerous tumor cell lines [11]. The principle kinds of Ag(I) complexes whose properties are improvingly stable and pharmacological might be sum up as N-bidentate with coordination compounds with [12]. An unremitting attention has been given to synthesizing more potent Ag(I) complexes having N-donor ligands with cytotoxic behaviour while showing minimum or no side effects in comparison with cis-platin [13]. This study stated how the synthesis, antimicrobial activity and cytotoxicity of new Ag(I) complexes with (E)-5-((E)-(1H-benzo[d]imidazol-2-yl)diazenyl)-N-(4-chlorobenzylidene)-4,6-dimethylpyridin-2-amine derivatives, are displaying higher cytotoxicity against PC3 cell. The Ag(I)-complexes also showed antitumor features with no nephrotoxic side-effects. Hence, this paper aims at exploring further structure-activity relations and discern anticancer drugs, the synthesis, characterization and cytotoxicity of new Ag(I)-complexes with Azo-schiff ligand are designated.

EXPERIMENTAL

Materials and Measurements

All chemicals and solvents manipulated in this paper were high purity provided from multiple companys such as Fluk, BDH, Aldrich and Sigma and used without further purification. Doubly distilled water was used in all experiments Elemental analysis of Azo-Schiff base dyes ligand and its metal complexes were implemented through micro analytical unit of EA 300 C.H.N Element analyzer. 1H - NMR spectra were recorded on a model Bruker 500 MHZ spectrophotometer using DMSO- d_6 as a solvent and TMS as an internal standard. Mass spectra was obtained using a shimadzu Agilent Technologies 5973C at 70° and MSD energy using a straight insertion of probe (Acq method 10 W energy) at temperature $90-110^\circ C$. Electronic spectra were measured in absolute ethanol

as a solvent (10^{-4}M) in the range (200-1100) nm by using a UV-Visb. T80-PG spectrophotometer. X-ray diffraction were measured using Bestec Germany Aluminium anode model X pertpro, wavelength of X-ray beam($\text{Cu } k_{\alpha}$) 1.54 angstrom, Anod material=Cu, the Voltage = 40KV and current = 30mA. Infrared spectra were recorded in KBr medium as discs using a shimadzu 8400 S FT-IR spectrophotometer in wave number at range (4000-400) cm^{-1} . SEM images of ligand and its complexes, were taken using micrograph kyky 3200. The magnetic susceptibility for the prepared metal complexes were measured at room temperature using faraday method. For this purpose, Burker Magnet (B.M) had been employed and the diamagnetic correction were made by pascals constants. TGA analysis were measured with England PL- TG using Rheometric scientific TGA-1000. Electric molar conductivity measurments were carried out at room temperature in DMF (10^{-3}M) solution by using conductivity bridge model 31A. The melting degrees of ligand and its complexes were measured by using electro thermal melting point 9300 .

Synthesis of Azo Ligand (L_1)

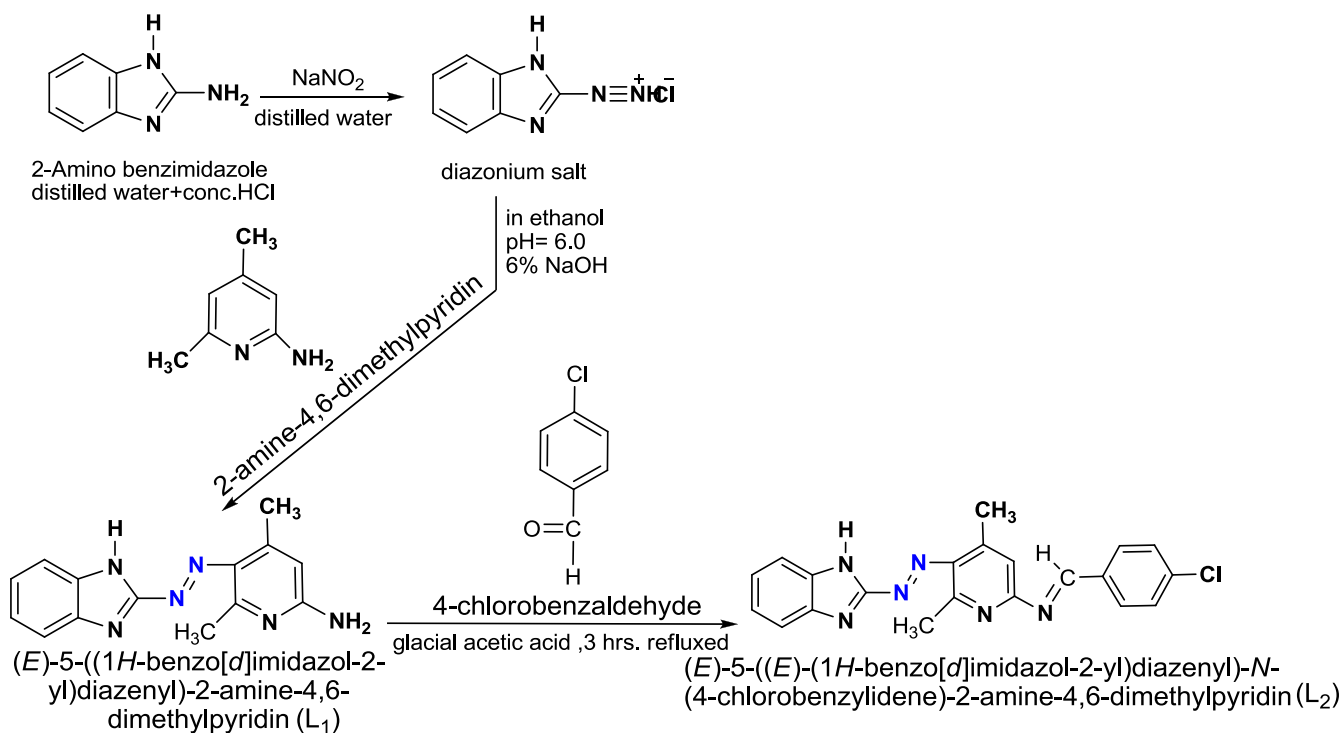
Azo ligand (L_1) was synthesized following the analogous procedure [14] and Al-Adilee *etal* [15] with some modification in a two-step process as described below. In the first step, 2-Amino benzimidazole (1 mmol) was mixed with hydrochloric acid 3ml in (30 mL) distilled water and diazotized below $5\text{ }^{\circ}\text{C}$ with sodium nitrite NaNO_2 (0.75 gm, 1 mmol, dissolved in 20 ml distilled water) was added in drops. In the second step the diazonium chloride compound was then coupled with 2-amine -4,6-dimethylpyridin in alkaline media below $5\text{ }^{\circ}\text{C}$. The pH value during the coupling was maintained between 6.5- 7.5 ,Coupling to the 4,6-dimethylpyridin-2-amine occurred at the *para*-position to the amine group (E)-5-((1H-benzo[d]imidazol-2-yl)diazenyl)-4,6-dimethylpyridin-2-amine (L_1).

Synthesis of Azo-Schiff base Ligand (L_2)

Numerous reaction ways are used to synthesize Schiff bases. An acid catalysed condensation reaction of amine and aldehyde or ketone which put under refluxing conditions is the most popular. To conduct this, firstly, a dose of nucleophilic nitrogen atom of amine on the carbonyl carbon, leading to typically uneven carbinolamine intermediate are used. Such reaction is capable of reversing to the initial materials, or when the hydroxyl group is removed and a $\text{C}=\text{N}$ bond is formed an imine can be molded. As amine is basic, it is regularly protonated in acidic conditions in very simple reaction settings the reaction is delayed as adequately protons are not accessible to catalyse the removal of the carbinolamine hydroxyl collection. General, aldehydes react quicker than ketones in Schiff base condensation reactions as the reaction focus of aldehyde is sterically less delayed than that of ketone. Additionally, the additional carbon of ketone contributes to the electron density and therefore creates the ketone less electrophilic than that of aldehyde .

the azo-schiff base ligand (L_2) was manufactured in terms of condensation method [16]. About (0.266 g, 1 mmol) of (L_1) in absolute ethanol (20 mL) was added drop-wise to hot absolute ethanol (50 mL) solution of 4-chlorobenzaldehyde (0.149 g, 1 mmol) with few drops of glacial acetic acid as a catalyst (Scheme-1). The mixture was refluxed and stirred magnetically for 2 hr. at $80\text{ }^{\circ}\text{C}$ after cooling, The solid product was filtered off, and washed several times with cold distilled water then dried in vacuum for several hours and recrystallized twice from hot ethanol to afford red coloured product and stored in a desiccator over anhydrous calcium chloride. Yield: 67 %; m.p. $159\text{ }^{\circ}\text{C}$

The purity was established by the elemental analysis and thin layer chromatography TLC techniques. The structure of azo schiff base ligand (L_2) is changed by $^1\text{H-NMR}$, mass spectrum, IR and UV-visb. spectra. The structural of the ligand (L_2) as shown below:



Scheme(1):- preparation of new azo-schiffbaes ligand (*L*₂)

Synthesis of Metal Complexes

The ligand *L*₂ 0.388 g (1 mmol) was dissolved in 25 ml methanol . The mixture was then refluxed for 60 minutes. A solution 1 mmol of Au(III) chloride salt in 25 ml methanol was added dropwise with stirring to the ligand solution. The resulting deep colour solution was refluxed for 60 minutes with stirring[17]. A deep colour precipitate formed compounds were filtered off, washed with absolute ethanol and recrystallized in ethanol. But Cu(II), and Ag(I) complexes were prepared by the addition of appropriate metal salts (0.5 mmol, dissolved in 30 ml hot buffer solution (ammonium acetate) at PH=7.0 for each metal ions to a solution of *L*₂ (1 mmol, in 20 mL absolute ethanol).The resulting solutions were refluxed for 1 h and then the volume of the solution was reduced to one-half by evaporation[18]. The precipitate was filtered off, washed with distilled water and washed with 5 ml ethanol to remove any traces of unreacted materials and dried in air. The % yield, m.p, color, molecular formula, M.wt and element analysis data (C.H.N) of ligand and its metal complexes are collected in table 1.

Table (1):- Analytical and physical data of ligand (*L*₂) and its metal complexes

compound	color	m.p °C	% Yield	Molecular Formula (Mol.wt)	Found (calc.)%			
					C	H	N	M
Ligand =(L ₂)		159	67	C ₂₁ H ₁₇ ClN ₆ (388.85)	65.14 (64.86)	4.50 (4.41)	21.88 (21.61)	----
[Cu(L ₂) ₂ Cl ₂].H ₂ O	Greenish blue	203	72	C ₄₂ H ₃₆ Cl ₄ CuN ₁₂ O (930.17)	54.46 (54.23)	3.97 (3.90)	18.43 (18.07)	7.11 (6.83)
[Ag(L ₂)(ONO ₂)(H ₂ O)]	Orange blush	181	63	C ₂₁ H ₁₉ AgClN ₇ O ₄ (576.74)	43.96 (43.73)	3.40 (3.32)	17.38 (17.00)	18.92 (18.70)
[Au(L ₂)Cl ₂]Cl	Purple red	194	76	C ₂₁ H ₁₇ AuCl ₄ N ₆ (692.18)	36.62 (36.44)	2.59 (2.48)	11.93 (12.14)	28.23 (28.46)

Result and Discussion

Characterization of azo –schiff base ligand (L₂) and its metal complexes

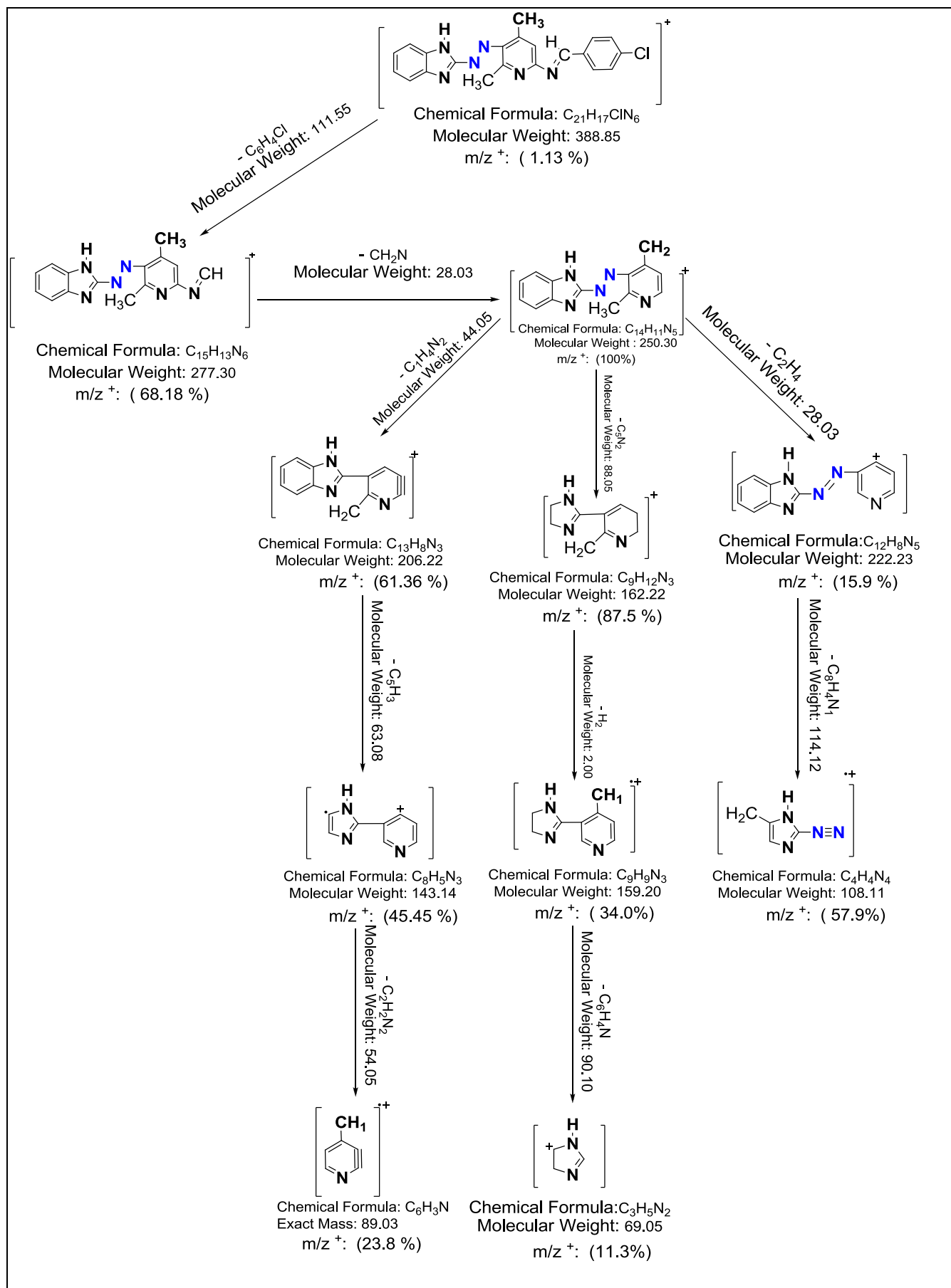
The analytical data of the complexes and some techniques such as infrared ,elemental analysis, mass spectrum, Uv–visib.spectroscopy and thermal analysis show that the (E)-5-((E)-(1H-benzo[d]imidazol-2-yl)diazenyl)-N-(4-chlorobenzylidene)-2-amine-4,6-dimethylpyridin (L₂) reacts with Cu(II) chloride in 1:2 (M:L) molar ratio to give the complexes of general composition [Cu(L₂)₂Cl₂].H₂O. But at react the ligand(L₂) with Au(III) chloride and Ag(I) nitrate exists in1:1 (M:L) molar ratio to give the metal complexes of general composition [Au(L₂) Cl₂] Cl and [Ag(L₂) (ONO₂)(H₂O)] respectively.

The complexes derived from azo schiff base ligand are stable toward air and insoluble in water and some common organic solvents but soluble in ethanol, methanol, dimethylformamide ,dimethylsulfoxide and acetone. Microanalytical data for the ligand and its metal complexes are in very good agreement with theoretical values.

¹H-NMR Spectra

In the ¹H NMR spectrum of azo-schiff base ligand (L₂) and Ag(I)-complex at ambient temperature in DMSO-d₆, with TMS as an internal reference, the ¹H NMR spectra of ligand(L₂) shows signals due to (NH) and(Ar-H) protons at δ=5.219 and δ= 8.375-6.906 ppm, respectively.The singlet at δ=9.059 ppm is due to the azomethine proton (–CH=N). A signal at δ=2.403 ppm assigned to solvent proton. signal at δ=2.796 and δ= 3.413 ppm is ascribed to methyl group[19].

In the spectrum of Ag(I) complex these signals were observed slightly change in the peak positions result the coordination of nitrogen atom of this group to Ag(I) ion. In the spectrum [Ag(L₂)(NO₃)(H₂O)] a signal is appeared in the range of δ=2.899- 3.418 ppm corresponding to –CH₃ and N-CH₃ protons. a signal is appeared in δ=5.169 corresponding to H₂O protons and multiplets around δ=6.891-8.167 ppm are assigned to aromatic protons. Signals corresponding to CH=N protons were observed in δ=8.498 ppm . A signal at δ=2.487ppm assigned to solvent proton[20].



Scheme 2. Mass spectrum fragmentation of ligand(L₂)

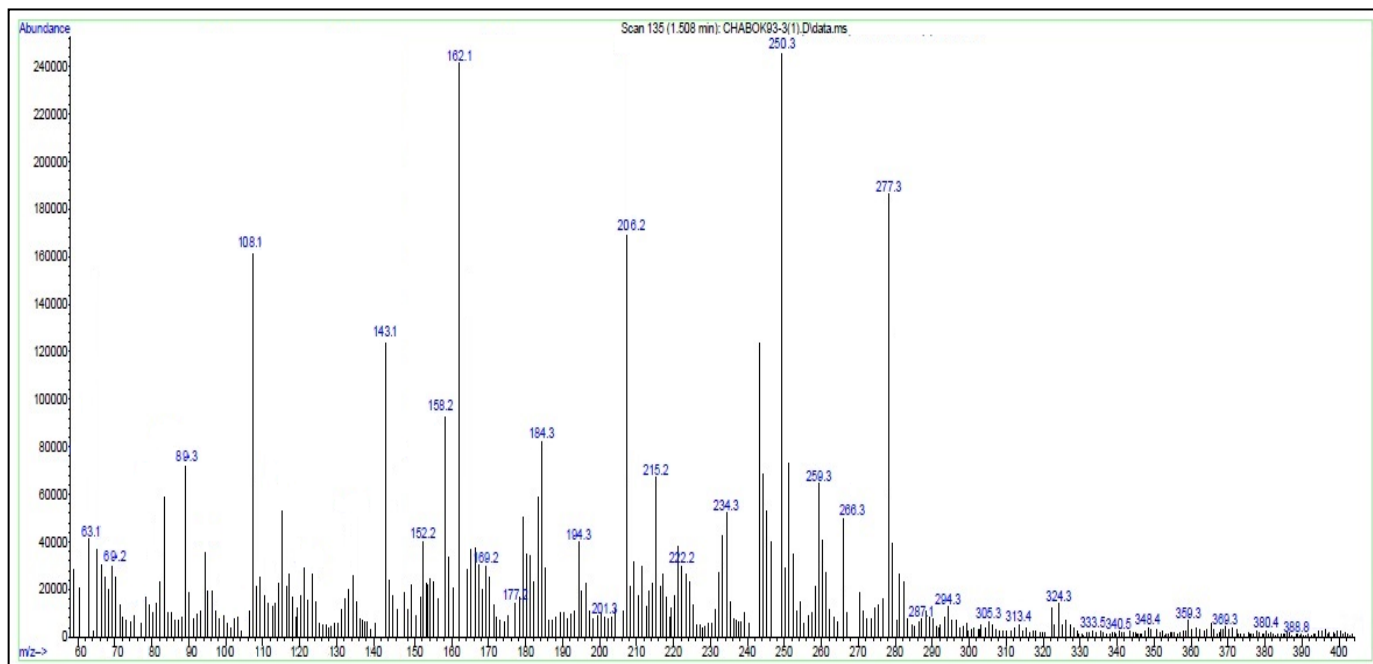
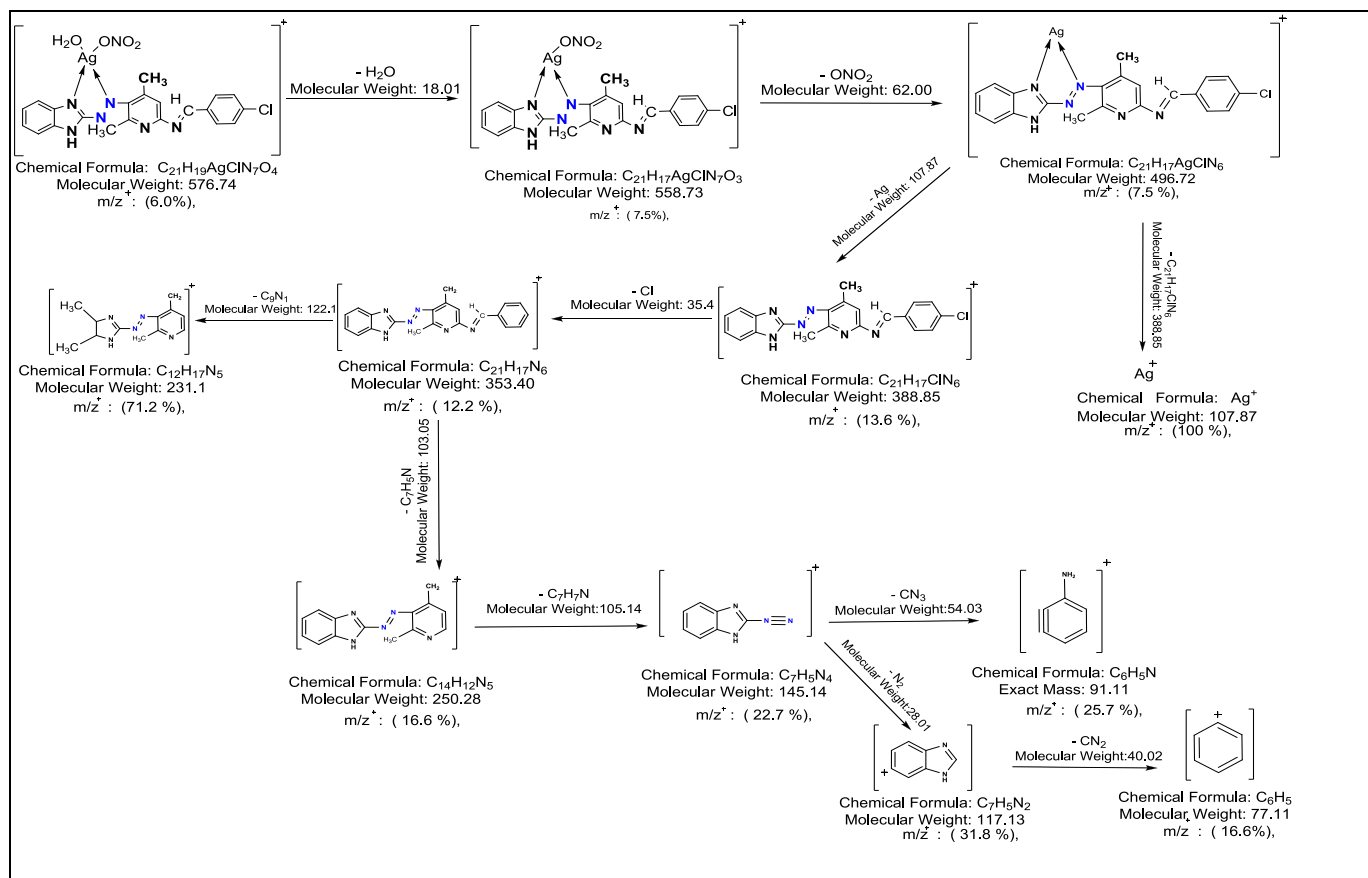


Figure (3):-Mass spectrum of azo –schiff base ligand (L₂)

The molecular ion peaks of Ag(I) - complex shows different m/z^+ values with different intensities. The mass spectra contain molecular ion peaks at m/z^+ 576.4, 558.7, 496.7, 388.8, 353.4, 250.3, 231.1, 145.1, 117.1, 107.8, 91.1 and 77.1 for structures respectively $[C_{21}H_{19}AgClN_7O_4]^+$, $[C_{21}H_{17}AgClN_7O_3]^+$, $[C_{21}H_{17}AgClN_6]^+$, $[C_{21}H_{17}ClN_6]^+$, $[C_{21}H_{17}N_6]^+$, $[C_{14}H_{12}N_5]^+$, $[C_{12}H_{17}N_5]^+$, $[C_7H_5N_4]^+$, $[C_7H_5N_2]^+$, Ag^+ , $[C_6H_5N]^+$ and $[C_6H_6]^+$. This data is in good agreement with the corresponding molecular formulae[22].



Scheme 3. Mass fragmentation of Ag(I)-Complex $[Ag(L_2)(ONO_2)(H_2O)]$

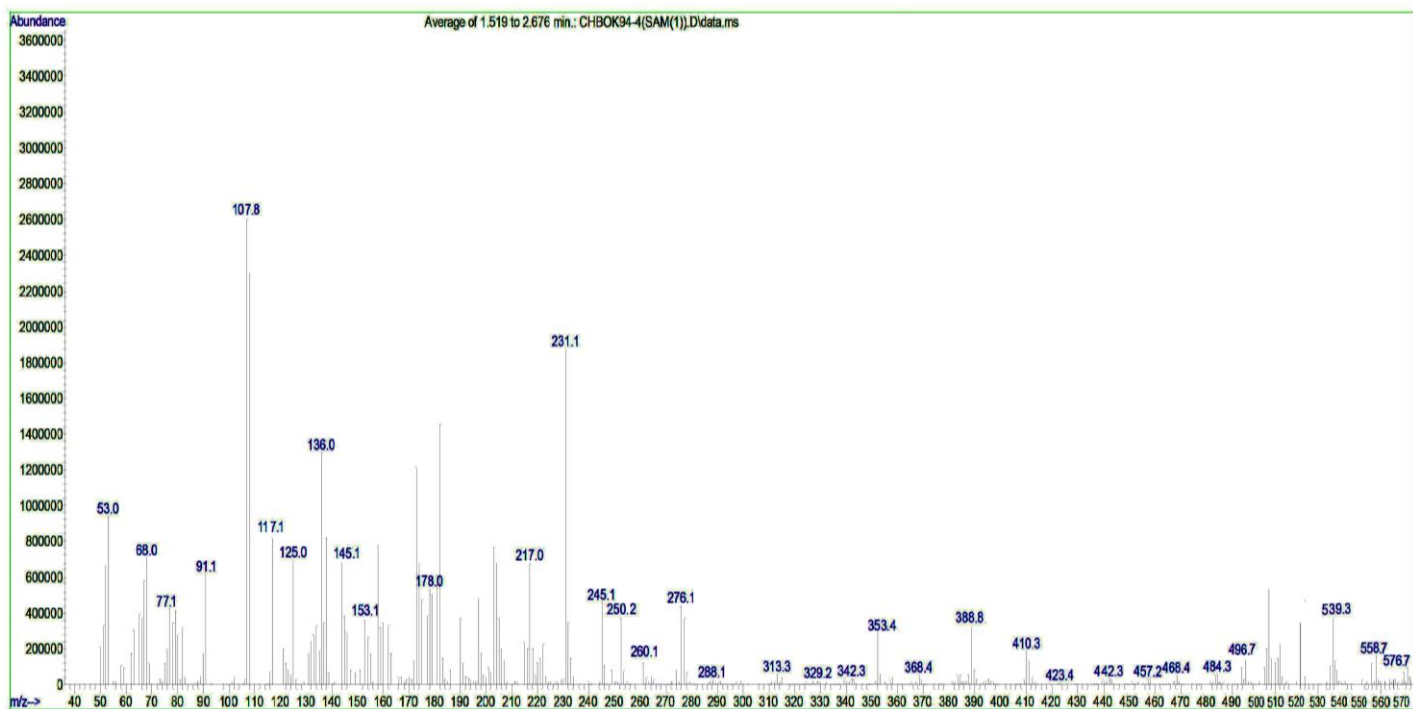
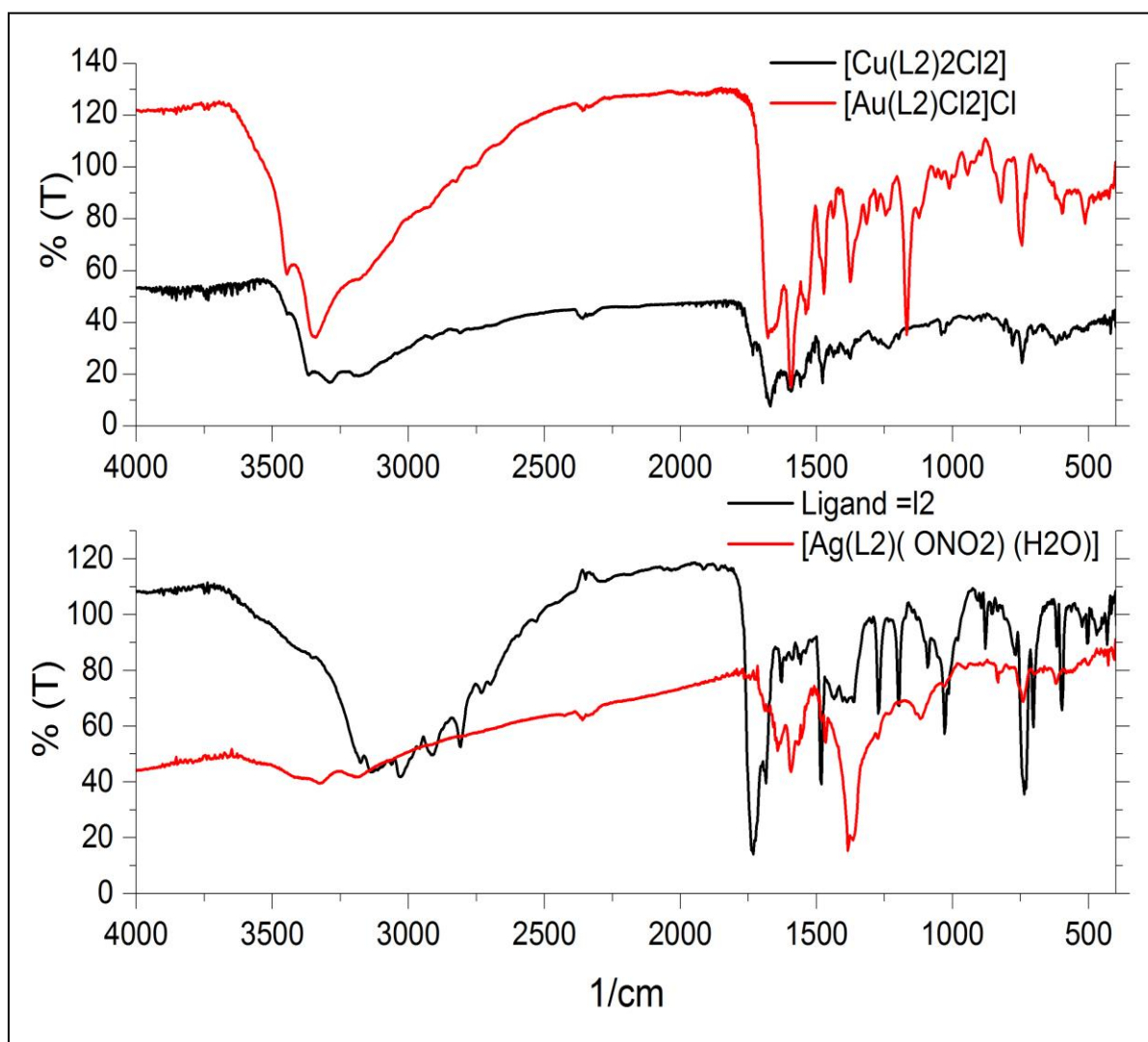


Figure (4):-Mass spectrum of Ag-Complex:[Ag(L₂)ONO₂.H₂O]

Infrared spectra of azo-schiff base ligand and their metal complexes

The important IR bands of ligand (L₂) and its complexes [Cu(L₂)₂Cl₂], [Ag(L₂) (NO₃) (H₂O)] and [Au(L₂)Cl₂]Cl are listed in Table 2. The IR spectra of the complexes are compared with those of the free ligand in order to determine the coordination sites that may be involved in chelation. There are some guide peaks, in the spectra of the ligand, which are of good help for achieving this goal. In the IR spectra of all the metal complexes, two sharp peaks observed in the region (1643-1685)cm⁻¹ and (1465-1481) cm⁻¹ are due to azo and azomethine (in benzimidazol ring) functions respectively. The absorption frequency of azo and azomethine (in benzimidazol ring) functions which have appeared at 1685 and 1481 cm⁻¹ in case of the ligand, have been shifted to lower frequency in all the metal complexes indicating the involvement of nitrogen atom of azo function and nitrogen atom of azomethine (in benzimidazol ring) function in complexation with the metal ions. The IR spectrum exhibits band at region (3132-3340) cm⁻¹ which may be assigned to (N-H) stretching vibration. The band of (C=N) asy in the IR spectra of the free ligand still lie at the same position in the IR spectra of the complexes. These indicate that these groups did not contribute to the coordination of the metal ions in the complexes. This is further confirmed by the appearance of new bands in the region 432-505 cm⁻¹ is due to ν M-N stretching vibrations in all the complexes [23,24].



Figure(5):-IR Spectrum of ligand and prepared metal complexes

Table (2):- Selected infrared absorption bands (4000-400) cm^{-1} for azo-schiff base ligand (L_2) and its metal complexes (KBr disc).

Compounds	$\nu(\text{N-H})$	$\nu(\text{C=N})$ azomethine	$\nu(\text{N=N})$	$\nu(\text{C=C})$	$\nu(\text{C-N})$	$\nu\text{H}_2\text{O}$ (outer- sphere coordination)	$\nu\text{H}_2\text{O}$ (inner - sphere coordination)	$\nu(\text{M-N})$
ligand (L_2)	3132m	1685s	1481s	1272s	1195s	-----	-----	-----
$[\text{Cu}(L_2)_2\text{Cl}_2] \cdot \text{H}_2\text{O}$	3284m	1670s	1477s	1375m	1197m	3365w	-----	447w
$[\text{Ag}(L_2)(\text{NO}_3)(\text{H}_2\text{O})]$	3178w	1643m	1465s	1365m	1118m	-----	3325w	459w
$[\text{Au}(L_2)\text{Cl}_2]\text{Cl}$	3340m	1677m	1473s	1377m	1168s	-----	-----	455w

L=ligand (L_2) , S = strong , m= medium , w = weak

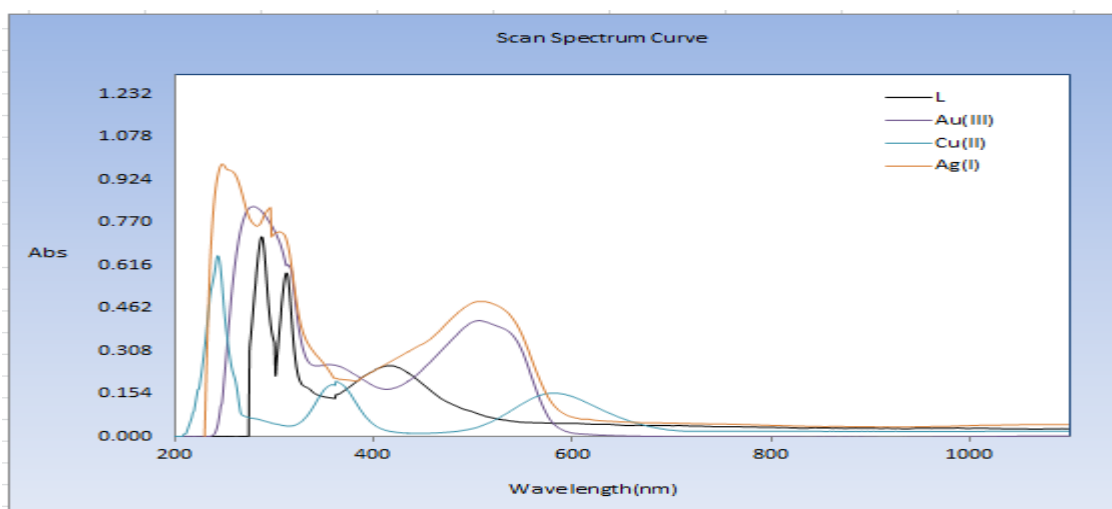
Magnetic susceptibility and electronic spectra measurements

The electronic spectra of ligand (L_2) and its complexes were measured in ethanol solvent at room temperature table 3 were recorded in ethanol solution, the spectrum of ligand (L_2) shows an intense absorption band at 417 nm (23980 cm^{-1}) assigned to $n \rightarrow \pi^*$ transition of azo and azomethine groups [25]. The geometries are supported by their electronic spectra.

The magnetic moment of the Cu(II)-complex has been found to be (1.78 B.M.), which is within the range of values corresponding to octahedral geometry. The spectrum of the Cu(II)-complex is consistent with the formation of an octahedral geometry with the appearance band centered at 576 nm (17361cm⁻¹), which may be assigned to ²E_g→²T_{2g} transition in an approximately octahedral environment and hybridization sp³d² [26].

Ag(I)-complex no d-d transition band of this complex exhibit high intense a charge transfer transition in visible region at 523 nm(19120cm⁻¹) which are due to (M→L,CT) [27] .The magnetic susceptibility for Ag(I)-complex due the electronic configuration d¹⁰ to be diamagnetic character (μ_{eff}=0.0B.M)which is characteristic of tetrahedral geometry at 1:1[M:L] and hybridization sp³ symmetry.

For Au(III)-complex , the spectrum shows one band at 516 nm(19379 cm⁻¹) due to ¹A_{1g}→¹B_{1g}(ν₁) transition. In is reasonable to suggest square planer configuration and hybridization dsp² (d⁸-low spin).The zero magnetic value of this complex (μ_{eff}=0.0B.M) indicate square planer geometry which is the common stereo chemistry for tetra coordinate Au(III)-complex[28].



Figure(6):- Absorption spectra of ligand (L₂) and its prepared metal complexes

Table(3):- Electronic spectra (nm , cm⁻¹), magnetic moments, geometry and hybridization

Compounds	λ _{max} (nm)	Absorption bands(cm ⁻¹)	Transitions	μ _{eff} (B.M)	Geometry	Hybridization
Ligand=(L ₂)	417	23980	n → π*	-----	-----	-----
	319	31347	π → π*			
	300	33333	π → π*			
[Cu(L ₂) ₂ Cl ₂].H ₂ O	576	17361	² E _g → ² T _{2g}	1.78	Octahedral distorted (Z-out or Z-in)	Sp ³ d ²
[Ag(L ₂) (NO ₃) (H ₂ O)]	523	19120	M→L,CT	dia	tetrahdra	Sp ³
[Au(L ₂)Cl ₂]Cl	516	19379	¹ A _{1g} → ¹ B _{1g}	dia	Square planer	dsp ² (Low spin)

B.M= Bohr magneton

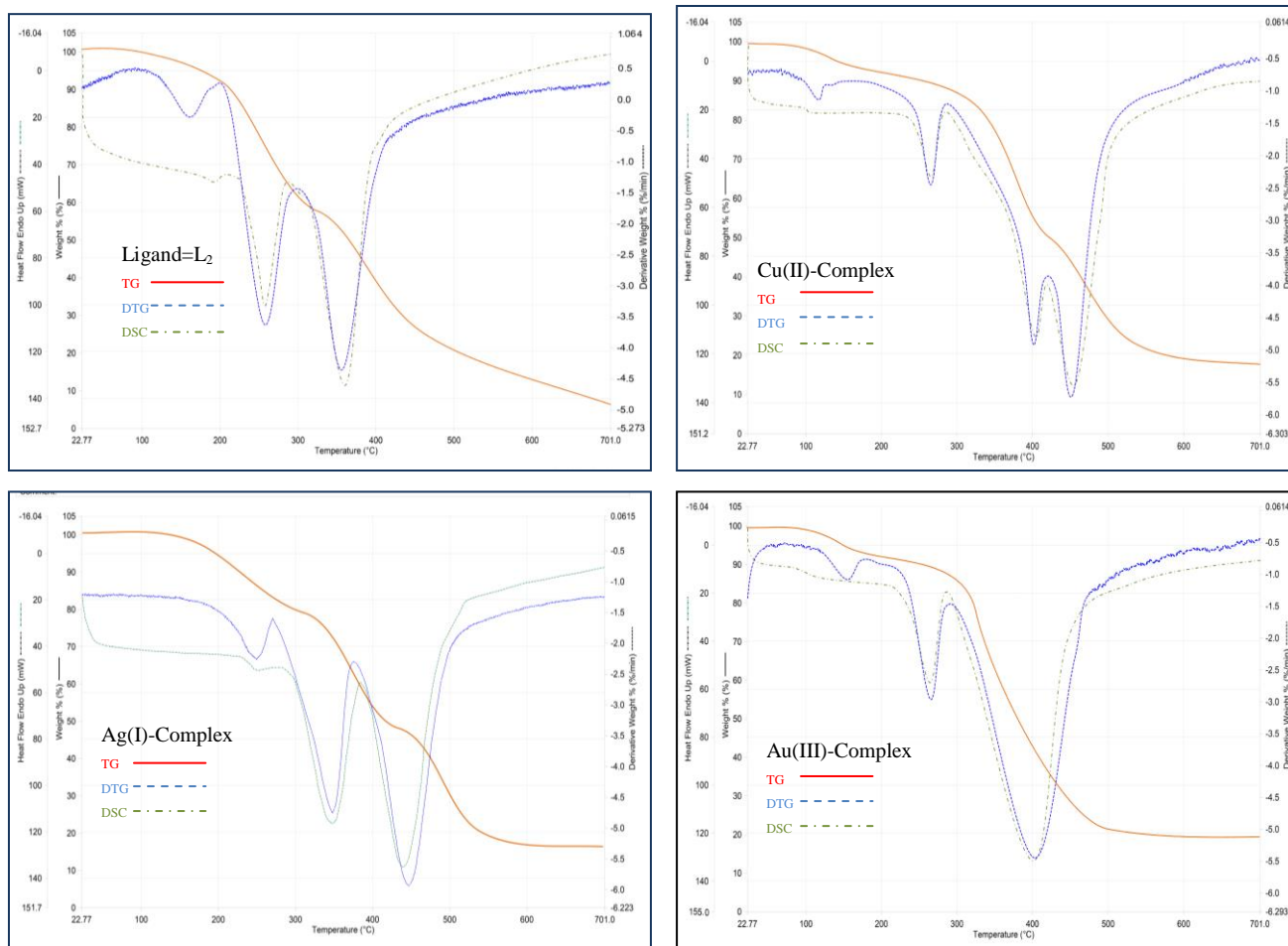
Thermal analysis

The thermal degradation of the azo Schiff base ligand and metal azo-Schiff base complexes were investigated by thermogravimetric (TG) analysis, differential thermogravimetric (DTG) and differential scanning calorimetry (DSC) in the temperature range 22-705 °C.

A representative TG,DTG,DSC diagram is given in Figure 7. The thermal stability data are listed in table 4. The data from the thermogravimetric analysis clearly indicated that the decomposition of the complexes proceeds in two, three or four steps. Water molecules were lost in first step between 50 - 200 °C and metal oxides were formed above 600 °C for complexes. The decomposition was complete at ≥ 600 °C for all complexes[29,30].

Table 4. Thermal analyses data for (TG,DTG,DSC) of ligand and metal complex.

Compound	Dissociation stages	Temperature Range (°C)	Mass loss Found (%)	DTG peak (°C)	DSC peak (°C)	Decomposition assignment	Residue
Ligand=L ₂	Stage I	100-700	92	155,360	189,367	The gradual loss of the ligand molecule	---
Cu(II)-complex	Stage I	90-149	4	119	109	The loss of the H ₂ O	CuO
	Stage II	149-330	18	283	282	The loss of the 2Cl molecule inner -sphere coordination	
	Stage III	330-600	83	403,452	411,458	The gradual loss of residual ligand	
Ag(I)-complex	Stage I	150-300	21.0	248	254	The loss of the H ₂ O and ONO ₂ molecule inner -sphere coordination	Ag ₂ O
	Stage II	300-600	82	246,459	248,447	The gradual loss of residual ligand	
Au(III)-complex	Stage I	127-200	6	151	120	The loss of the Cl molecule outer-sphere coordination	Au ₂ O ₃
	Stage II	200-330	20	260	263	The loss of the 2Cl molecule inner -sphere coordination	
	Stage III	330-600	80	406	410	The gradual loss of residual ligand	



Figure(7) :-TG-DTG-DSC curves of ligand (L₂) and its metal complexes

According to these results and discussed the data through different techniques suggest the structural formula of prepared metal complexes in this work may be proposed in figures (8-10) , shown below :-

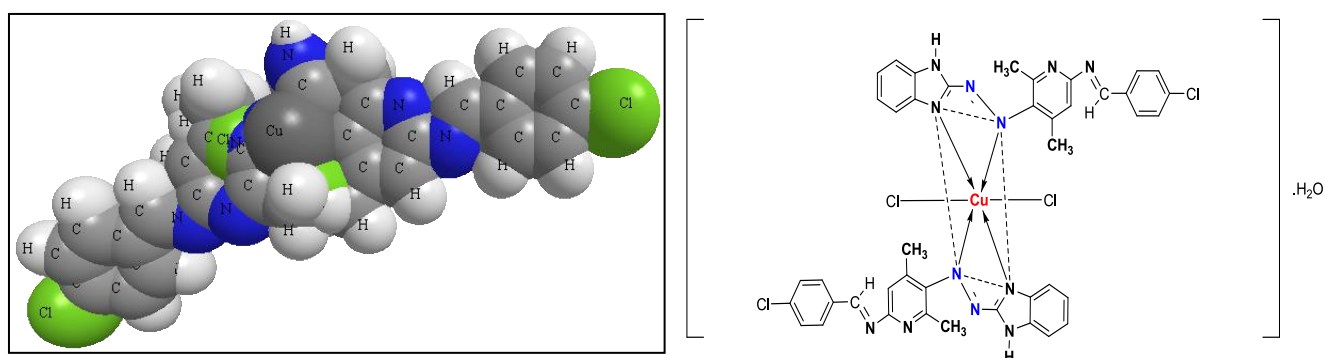


Figure (8):-The proposed chemical structure formula of the Cu(II)- complex

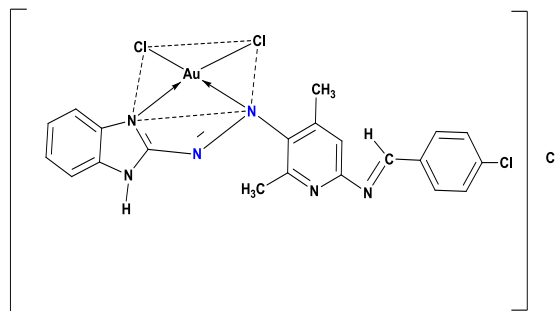
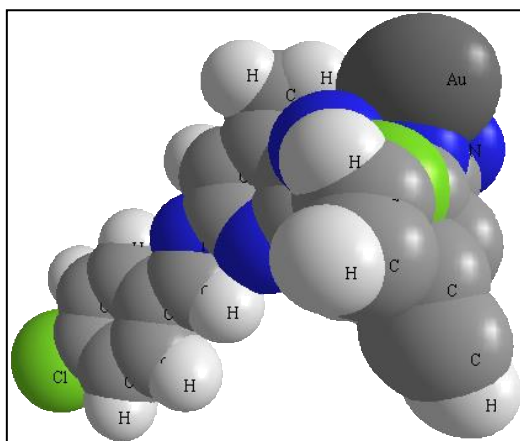


Figure (9):-The proposed chemical structure formula of the Au(III)-complex

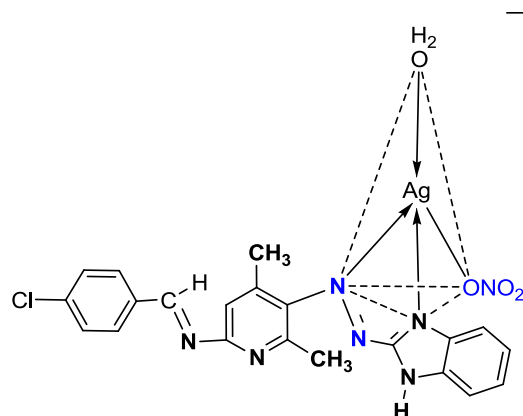
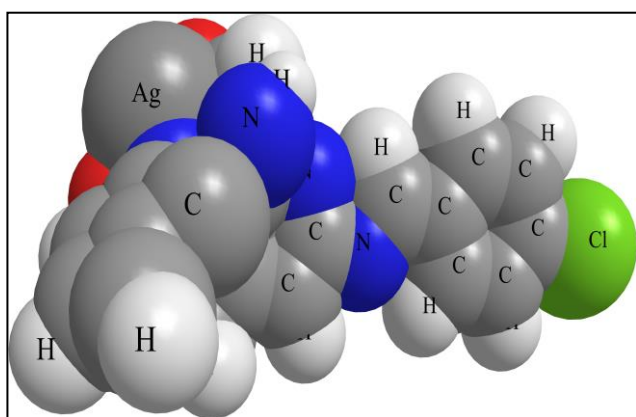


Figure (10):-The proposed chemical structure formula of Ag(I)-complex

X-ray diffraction analysis

The X-ray diffraction, XRD, patterns of the azo cshiff base ligand (L_2) and its metal complexes $[Cu(L_2)_2Cl_2] \cdot H_2O$, $[Ag(L_2)(NO_3)(H_2O)]$ and $[Au(L_2)Cl_2]Cl$, are shown in [figure 11](#). The XRD patterns of the azo-cshiff base ligand (L_2) and its metal complexes have sharp diffraction peaks at around $2\theta = (30-80)$, this indicates that azo-cshiff base ligand (L_2) and complexes are a mixture of crystalline and amorphous phases. While the XRD pattern of Au(III)-complex is very less mixture of crystalline and amorphous phase. cacluclate d-spacing or 'd' values of reflections were obtained using Bragg's equation $n\lambda = 2d \sin \theta$, The average size of the particles and their size distribution were evaluated by the Scherer equation, $D = k\lambda / \beta \cos \theta$ [31,32], The values in table 5

Table (5):- Inter planar distances , 2θ value, FWHM, Crystallite Size and Lattice Strain of each peak, relative intensity for ligand and complexes

Compound	2θ Obs. (degree)	d calc. spacing(\AA°)	FWHM [$^\circ 2\theta$]	Crystallite Size D(nm)
Ligand= L_2	32.487	2.753	0.173	0.815
	45.488	1.992	0.131	1.121
	56.547	1.626	0.102	1.508
Cu(II)-complex	32.188	2.778	0.112	1.259
	45.414	1.995	0.213	0.689
	46.086	1.968	0.134	1.098
	56.547	1.626	0.149	1.032
Ag(I)-complex	32.337	2.716	0.112	1.373
	45.264	2.001	0.113	1.299
	56.547	1.626	0.118	1.303
Au(III)-complex	32.188	2.778	0.231	0.610
	45.040	2.011	0.248	0.591

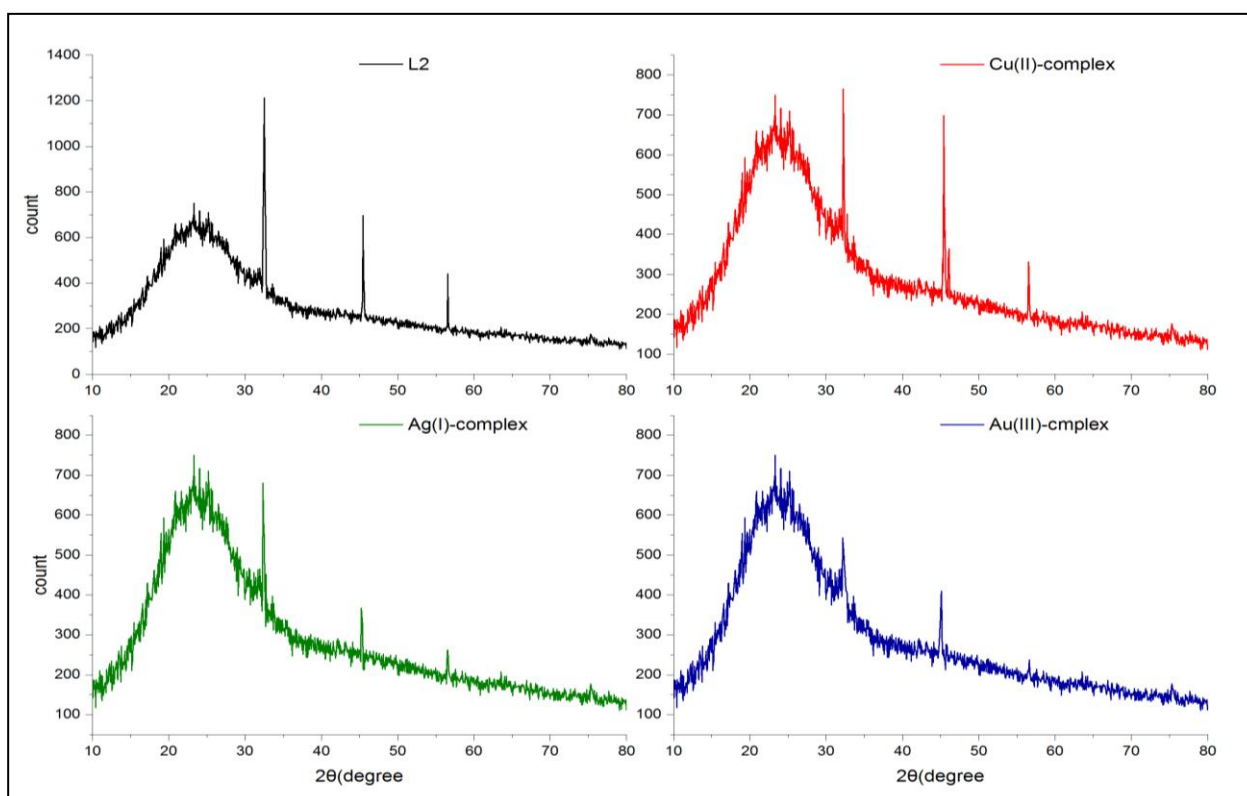


Figure (11):- X-ray diffraction patterns for ligand (L_2) and its metal complexes.

SEM studies

SEM is an easy method that might be manipulated to testify the deposited samples which obviously denoted how the nanoparticles have been shaped [33]. The images of SEM show that the diameters of the azo-schiff base ligand (L_2) and $[\text{Ag}(L_2) (\text{NO}_3) (\text{H}_2\text{O})]$

are about (50.4) and (106.7)nm, respectively. Figure 12,13 show the scanning electron microscopy pictures of azo-schiff base ligand (L_2) and $[Ag(L_2)(NO_3)(H_2O)]$.

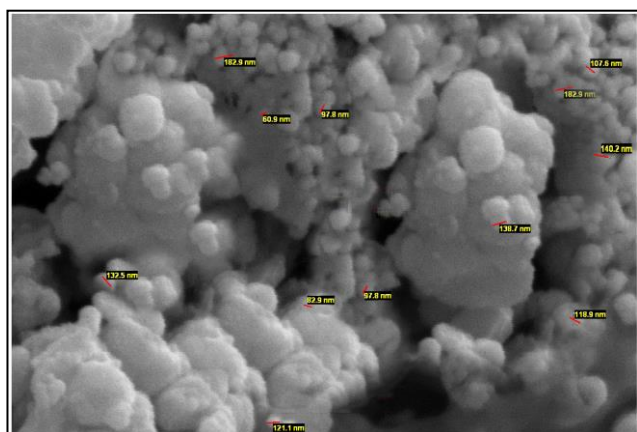


Figure. 13. Scanning electron micrographs of $[Ag(L_2)(NO_3)(H_2O)]$.

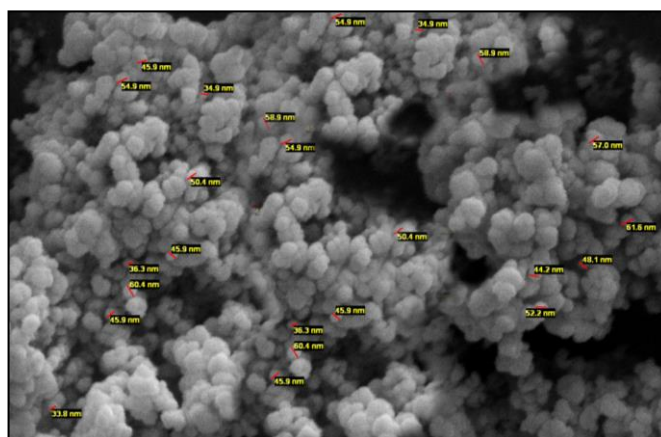


Figure. 12. Scanning electron micrographs of azo-schiff base ligand.

Pharmacolog results:-

Antibacterial activity

The synthesized compounds were tested for their inhibitory effects on the growth of bacteria *Staphylococcus aureus* representing Gram-positive bacteria and Gram-negative bacteria *Escherichia coli*. The results of the antimicrobial activity of the ligand and its metal chelates against all tested bacterial and fungal strains are shown in figure 14. The data of antimicrobial screen demonstrate that the compounds show antimicrobial properties. It is also significant to observe that the metal chelates display greater inhibitory effects than that of the parent ligand (L_2). Herein, the domain of inhibition is obviously much higher for metal complexes against the selected bacterial strains than the free ligand (L_2). The amplified behaviour of the metal chelates might be understood in terms of the chelation theory. The activity of the chelation inclines to instigate the ligand to behave with extra power and potency as bactericidal agents, therefore; their killing action to the tested bacterial strains is more than that of the free ligand. The experimental observation on a complex suggests that the positive charge of the metal is partly joint with the donor atoms which are in the ligand, and there might be π -electron delocalization over the complete chelating. This rises the lipophilic feature of the metal chelate, infusing it through the lipid cover of the bacterial membranes. Since the tested complexes were observed to be more active against Gram-positive than Gram-negative bacteria, it might be concluded that the antimicrobial activity of the compounds is associated with the structure of the bacteria cell wall. To explain this, the wall of the cell is indispensable to the existence of bacteria. The process of kill bacteria for some antibiotics is incurred by impeding a stage in the peptidoglycan synthesis. While Gram-positive bacteria have a thick cell wall comprising several layers of peptidoglycan and teichoic acids, Gram negative bacteria possess a comparatively thin cell wall which is containing a few layers of peptidoglycan, bounded by a second lipid membrane comprising lipopolysaccharides and lipoproteins. Accordingly, The differences in the structure of the cell wall might lead to differences in antibacterial vulnerability and some antibiotics can kill only Gram-positive bacteria and is infective against Gram-negative pathogens. Solubility, conductivity, and bond length between the metal and the ligand are some of the other aspects that might increase this activity[34].

Antifungal

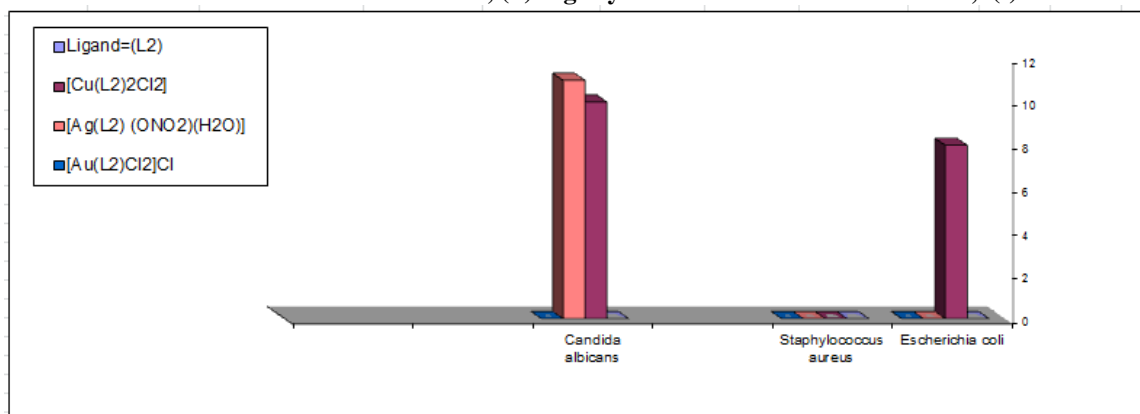
The antifungal activity of ligand and its complexes have been studied by agar diffusion method against the fungi *Alternaria*. Flucanazole is used as standard antibiotic and DMSO

is used as solvent [35]. The antifungal activity of the azo-schiff base and metal complexes against the fungi *Alternaria* are shown in Table 6 and figure 14

Table(6):-Antibacterial activity of ligand (L₂) and its metal complexes

Compounds	Anti - bacterial Activity		Anti - fungal Activity
	<i>E. coli</i>	<i>Staphylococcus</i>	<i>Alternaria</i>
Ligand=(L ₂)	-	-	-
[Cu(L ₂) ₂ Cl ₂] .H ₂ O	+	-	++
[Ag(L ₂) (ONO ₂)(H ₂ O)]	-	-	++
[Au(L ₂)Cl ₂]Cl	-	-	-

(++) Moderate active-Inhibition zone=9-12mm, (+)Slightly active-Inhibition zone=6-9mm, (-)Inactive <6mm.



Figure(14):- Minimum Inhibitory concentration (MIC) in molar concentration (10⁻⁴ M) of the ligand (L₂) and its metal complexes

Mechanism of azo – schiff base reduction

The first step in the bacterial degradation of azo –schiff base dye in either aerobic or anaerobic condition is to reduce the –N=N– bond. Reduction may be due to enzymes, redox mediator, and chemical reduction by reductants like sulfide or combination. This reaction involving enzyme-mediated azo dye reduction may be either specific or nonspecific to dye. The presence of azo reductase in anaerobic bacteria was first reported by Rafii et al. in *Clostridium* and *Eubacterium*. Azo reductase from these strains were oxygen sensitive and were formed constitutively and released extracellularly. Later investigation made by Rafii and Cernglia has shown azo reduction in *Clostridium perfringens* by an enzyme FAD dehydrogenase. The gene for this enzyme for *C. perfringens* has been cloned and expressed in *Escherichia coli*. Another mechanism of dye decolorization could involve cytosolic flavin-dependent reductions, which transfer electron via soluble flavins to azo dyes. However, recently Russ et al. have shown that recombinant *Sphingomonas* strain BN6 could reduce sulfonated azo dyes by cytosolic flavin-dependent azo reduction in vitro and not in vivo [36].

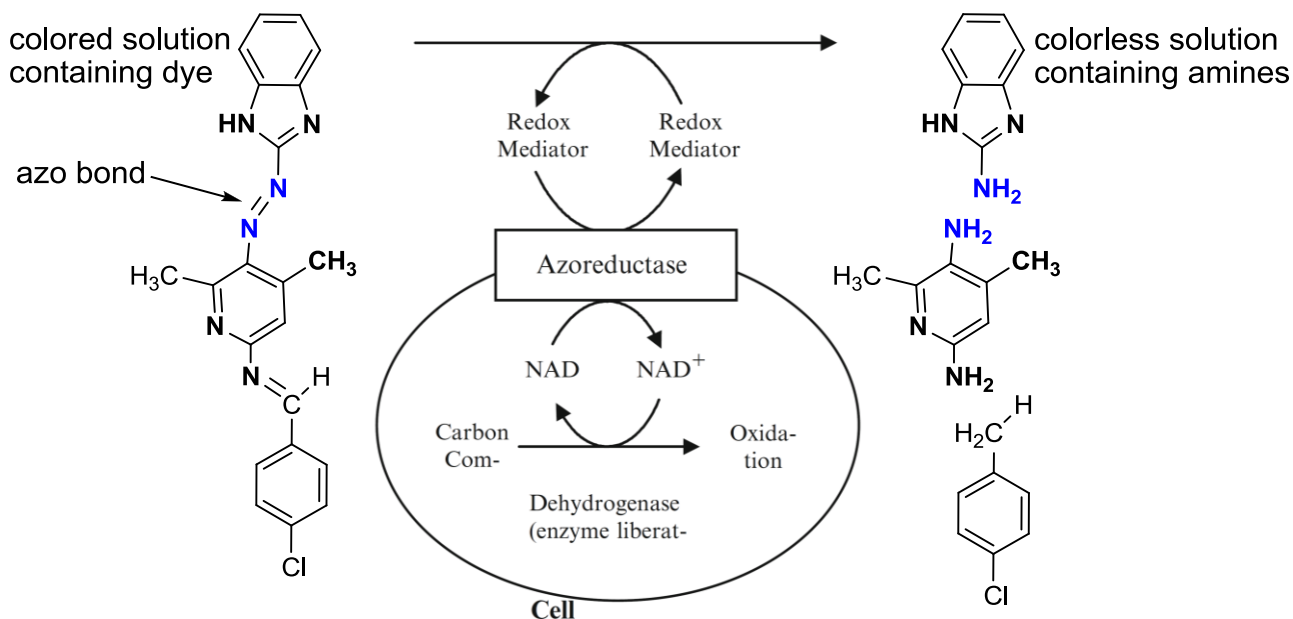


Figure (15):- Possible mechanisms for the removal of azo -schiff dyes by bacteria

Cell viability and cytotoxicity assay

Antiproliferative efficacy of the synthesized compounds was evaluated using MTT assay. The assay plates were read using a microplate reader at an absorbance wavelength of 570 nm. 0.1% DMSO was used as negative control. Tamoxifen and 5-fluorouracil were used as standard reference drugs against PC3 cells. The selectivity index (SI), which indicates the cytotoxic selectivity of the compound against cancer cells and its safety towards the normal cells was determined from the ratio of the IC_{50} obtained from the test on normal cell versus the IC_{50} for cancer cell. Whereas, IC_{50} (median inhibitory concentration is the concentration which causes 50% inhibitory effect on cellular proliferation) values were estimated using regression equation obtained from the dose-response curve [37].

One cancer cells namely (PC3) cancer cell lines were used to determine the antiproliferative effect of synthesized compound. In addition, an WRL, was also used as a model for normal cells line. The compound 5-fluorouracil were used as positive controls. The median inhibitory concentration (IC_{50}) values were calculated for each cell line Table 7. Compound $[Ag(L_2)(ONO_2)(H_2O)]$ showed selective cytotoxicity against cancer cell line PC3 with $IC_{50} = 246 \mu M$, while it was safe on WRL with $IC_{50} = 5803 \mu M$, for normal human cells

Table(7):- IC₅₀ (µg/ml) values and percentage (%) of the synthesized compound and standard drugs

Test samples	IC ₅₀ (µg/ml)			
	Carcinoma Cell Lines		Normal Cell Line	
[Ag(L ₂)(ONO ₂)(H ₂ O)]	246.092		5803.548	
	Mean Percentage (%) for each cell line			
Conc. (µg/ml)	Carcinoma Cell Lines		Normal Cell Line	
	Cell Viability	Cell Inhibition	Cell Viability	Cell Inhibition
400	27.432	72.568	73.605	26.395
200	59.68367	40.31633	85.84133	14.15867
100	78.62667	21.37333	93.827	6.173
50	90.97233	9.027667	97.37667	2.623333
25	86.92133	13.07867	95.139	4.861
12.5	92.86267	7.137333	92.631	7.369
6.25	95.602	4.398	94.94567	5.054333

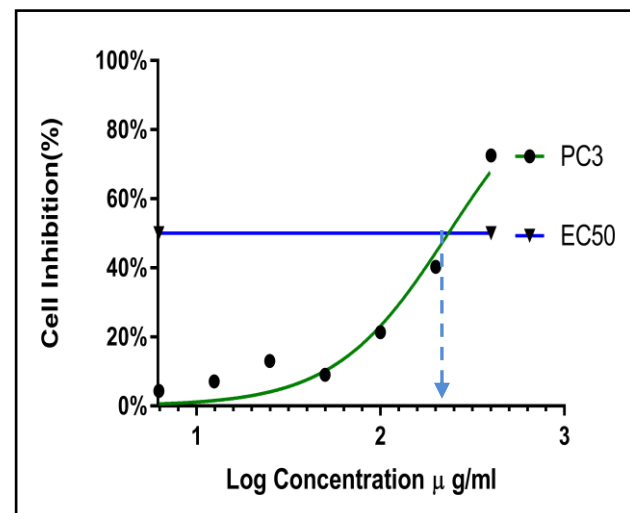
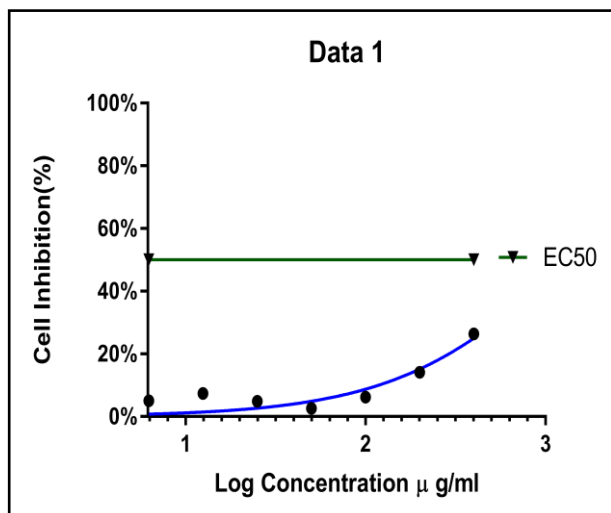
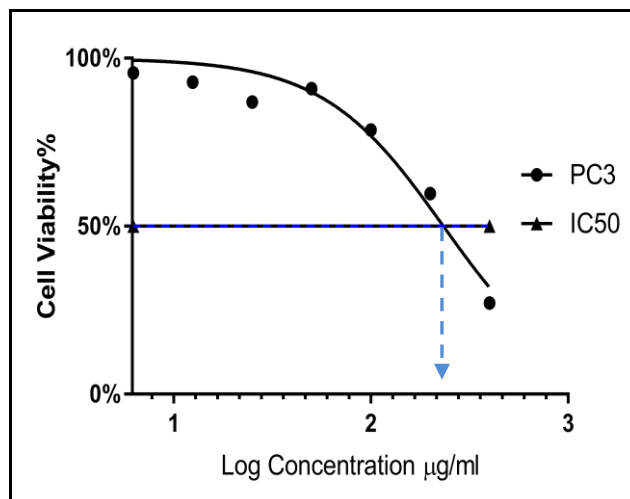
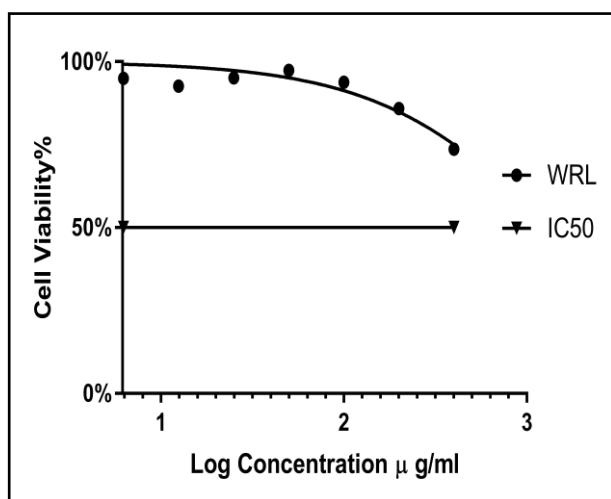


Figure (17):- EC₅₀ (µg/ml) values of the carcinoma cell lines and normal cell Line.

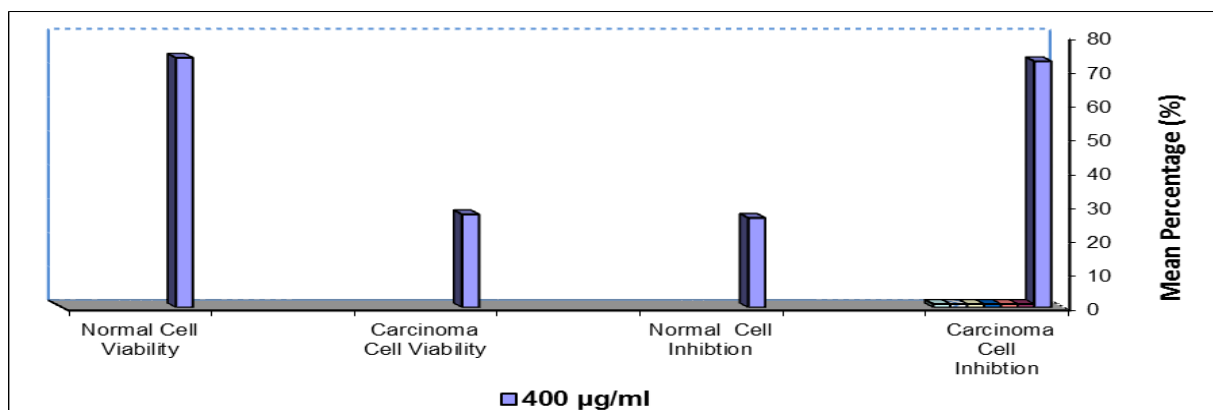


Figure (18):- Comparison of viability and Inhibition for each cell line (10000 cellular density)

Conclusion

In the present study, Azo-schiff base ligand (L_2) and its complexes $[Cu(L_2)_2Cl_2]$, $[Ag(L_2)(ONO_2)(H_2O)]$ and $[Au(L_2)Cl_2]Cl$ were synthesized and characterized. The antibacterial activity of the prepared complexes was also studied against gram positive and gram negative bacteria. It is found that some of the complexes are quite effective against tested bacteria. The complex $[Ag(L_2)(ONO_2)(H_2O)]$ demonstrated more pronounced anti-cancer efficacy against human prostate cancer cells with median inhibitory concentration (IC_{50}) values. In addition, the complex $[Ag(L_2)(ONO_2)(H_2O)]$ demonstrated higher selectivity index towards the tested cancer cells, while presenting safety profile towards the normal cells. From the findings of the present study, it can be concluded that the complexes of the Azo-schiff base ligand possess strong cytotoxic property and selectivity against human prostate tumour cells.

References

1. Munire Sarigul, Aysel Sari, Muhammet Kose, Vickie McKee, Mahfuz Elmastas, Ibrahim Demirtas, Mukerrem Kurtoglu, *Inorganica Chimica Acta*, S0020-1693(2015)1-33.
2. Serhan Uruş, Hamza Adigüzel, Mahmut İncesu, *Chemical Engineering Journal*, S1385-8947(2016)1-26.
3. M.A. Diab, A.Z. El-Sonbati, A.A. El-Bindarya, Sh.M. Morgan, M.K. Abd El-Kader, *Journal of Molecular Liquids*, 218 (2016) 571–585.
4. Tatjana Lazarević, Ana Rilakb and Živadin D. Bugarčić, *European Journal of Medicinal Chemistry*, S0223-5234(2016)1-73.
5. Simona Rubino, Rosalia Busà, Alessandro Attanzio, Rosa Alduina, Vita Di Stefano, Maria Assunta Girasolo, Santino Orecchio, Luisa Tesoriere, *Bioorganic & Medicinal Chemistry*, S0968-0896(2017)1-25.

6. Camilla Abbehausen a, Suelen F. Sucena a, Marcelo Lancellotti b, Tassiele A. Heinrich dEmiliana P. Abrod, Claudio M. Costa-Neto d, André L.B. Formiga c, Pedro P. Corbi a, ***Journal of Molecular Structure***, 1035 (2013) 421–426.
7. McCauley, J., Zivanovic, A. and Skropeta, D., ***Methods in Molecular Biology***, 1055 (2013) 191-205.
8. Sampriti Katak, Samarendra Hazarika and D.C. Baruah , ***Journal of Environmental Management*** 196 (2017) 201-216.
9. Daria Niedzielska, Tomasz Pawlak, Maria Bozejewicz, Andrzej Wojtczak, Leszek Pazderski and Edward Szlyk, ***Journal of Molecular Structure***, 1032 (2013) 195–202.
10. Tatjana Lazarević, Ana Rilak, Dr., Živadin D. Bugarčić, Prof. Dr., ***European Journal of Medicinal Chemistry***, S0223-5234(2017)1-79.
11. J. Joseph, G. Boomadevi Janaki, ***Journal of Photochemistry & Photobiology, B: Biology*** 162 (2016) 86–92.
12. Shen Li, Run-Jiang Song, Dong-Hui Wangb, Xue Tian, Xu-Sheng Shao, Zhong, ***Chinese Chemical Letters***, 27 ,(2016), 635–639.
13. Simona Rubino, Rosalia Busà, Alessandro Attanzio, Rosa Alduina, Vita Di Stefano, Maria Assunta Girasolo, Santino Orecchio and Luisa Tesoriere, ***Bioorganic & Medicinal Chemistry***,(2016), S0968-0896(16)1-25.
14. A.Z. El-Sonbati, M.A. Diab, A.A. El-Bindary, A.F. Shoair, N.M. Beshry , ***Journal of Molecular Liquids***, 218 (2016) 400–420.
15. Khalid J. Al-Adilee and Shaimaa Adnan, ***Oriental Journal of chemistry***, 33(4),(2017), 1-13.
16. Khalid J. AL-adilee and Haider M. Hessoon ***J. Chem. Pharm. Res.***, 7(8), (2015), 89-103.
17. Akkharadet Piyasaengthong, Nonlawat Boonyalai, Songwut Suramitr and Apisit Songsasen , ***Inorganic Chemistry Communications***, 59 (2015) 88–90.
18. B. Kulyk*, D. Guichaoua, A. Ayadi, A. El-Ghayoury, B. Sahraoui, ***Organic Electronics***, 36 (2016) 1-6.
19. Khalid J. AL-Adilee, H.A.H. AL-Shamsi and M.N. Dawood, ***Res. J. Pharm. Bio. Chem. Sci.***, 7(4) (2016).
20. Cihan Kantar, Vildan Mavi, Nimet Baltaş, Fatih İslamoğlu, Selami Şaşmaz, ***Journal of Molecular Structure***,(2016), S0022-2860(16)1-40.
21. R. Mathammal, K. Sangeetha, M. Sangeetha, R. Mekala, S. Gadheeja, ***Journal of Molecular Structure***, 1118 (2016) 316-324.

22. S. Demir, A. Guder, T. K. Yazıcılar, S. Çağlar, O. Buyukgungor, **Spectrochim. Acta, Part A** 150 (2015) 821–828.
23. Sujan Biswas, Samik Acharyya, Deblina Sarkar, Saswati Gharami, Tapan Kumar Mondal , **spectrochimica acta** ,(2016)S1386-1425(16)1-25 .
24. Khalid J.AL-Adilee, *Research Journal of Pharmaceutical, Biological and Chemical Sciences*, 6 ,(2015),1297.
25. A. Mostafa, N. El-Ghossein, G.B. Cieslinski, H.S. Bazzi, **Journal of Molecular Structure**. 1054–1055 (2013) 199-208.
26. Özlem Özdemir, **Journal of Molecular Structure**,(2016), S0022-2860(16)1-46.
27. A.A. El-Bindary a, A.Z. El-Sonbati a, M.A. Diaba, M.M. Ghoneim b, L.S. Serag a, **Journal of Molecular Liquids**, 216 (2016) 318–329.
28. Khalid J.AL-Adilee, Abass, A.K. and Taher, A.M. ,**Journal of Molecular Structure**, 1108,(2016), 378-397.
29. A.Z. El-Sonbati, M.A. Diab, A.A. El-Bindarya, G.G. Mohamed, S.M. Morgan, M.I. Abou-Dobara, S.G. Nozh, **Journal of Molecular Liquids** ,215 (2016) 423–442.
30. D. Karaagaç, G.S. Kürkçüoğlu, **Journal of Molecular Liquids**, 1105 (2016) 263-272.
31. Khalid J. Al-Adilee and Hussein A.K. Kyhoiesh, **Journal of Molecular Structure**, 1137(2017),160-178.
32. M. Shakir, S. Hanif, M.A. Sherwani, O. Mohammad, S.I. Al-Resayes, **Journal of Molecular Liquids**, 1092 (2015) 143–159.
33. Motaleb Ghasemian, Ali Kakanejadifard, Tahereh Karami, **spectrochimica acta** ,(2016) S1386-1425(16)1-44.
34. Simona Rubino, Rosalia Busà, Alessandro Attanzio, Rosa Alduina, Vita Di Stefano, Maria Assunta Girasolo, Santino Orecchio, Luisa Tesoriere, **Bioorganic & Medicinal Chemistry**,(2017), S0968-0896(16)1-25.
35. Yi Gou, Jinlong Li, Boyi Fan, Bohui Xu, Min Zhou, Feng Yang, **European Journal of Medicinal Chemistry**,(2017), S0223-5234(17)1-39.
36. Dr. Hatice Atacag Erkurt, **Biodegradation of Azo Dyes Springer**, Heidelberg Dordrecht London New York 2010.
37. Alberta Bergamoa and Gianni Sava*ab, **Chem. Soc. Rev.**,(2015),10.1039/c5cs00134j, 1-7.